

# Magnetoconductance of a two-dimensional metal in the presence of spin-orbit coupling

P. Schwab<sup>(1)</sup> and R. Raimondi<sup>(2)</sup>

<sup>(1)</sup>*Institut für Physik, Universität Augsburg, D-86135 Augsburg*

<sup>(2)</sup>*NEST-INFM e Dipartimento di Fisica, Università di Roma Tre, Via della Vasca Navale 84, 00146 Roma, Italy*

(November 13, 2018)

We show that in the metallic phase of a two dimensional electron gas the spin-orbit coupling due to structure inversion asymmetry leads to a characteristic anisotropy in the magnetoconductance. Within the assumption that the metallic phase can be described by a Fermi liquid, we compute the conductivity in the presence of an in-plane magnetic field. Both the spin-orbit coupling and the Zeeman coupling with the magnetic field give rise to two spin subbands, in terms of which most of the transport properties can be discussed. The strongest conductivity anisotropy occurs for Zeeman energies of the order of the Fermi energy corresponding to the depopulation of the upper spin subband. The energy scale associated with the spin-orbit coupling controls the strength of the effect. More in particular, we find that the detailed behavior and the sign of the anisotropy depends on the underlying scattering mechanism. Assuming small angle scattering to be the dominant scattering mechanism our results agree with recent measurement on Si-MOSFET's in the vicinity of the metal-insulator transition.

## I. INTRODUCTION

In recent years the transport properties of two-dimensional (2D) electron systems in Si-MOSFETs and semiconductor heterostructures have been the subject of a great deal of theoretical and experimental activity. One reason of this is the possibility of a metal-insulator transition (MIT) as the density of the 2D system is varied [1]. A “critical” density identified by a weakly temperature dependent resistivity separates an “insulating” region from a “metallic” one. In the latter, upon lowering the temperature roughly below 1K, the resistivity drops by almost one order of magnitude, whereas in the former the resistivity increases quickly. The origin of the MIT is still unclear and there is a wide debate in the literature concerning the relevance of the possible mechanisms. For recent reviews on the subject one may see Ref. [2] and [3].

On the insulating side the resistance resembles Efros-Shklovskii hopping [4], which points towards the relevance of localized states and a soft gap in the density of states; also the thermopower has been interpreted in terms of an Anderson insulator [5]. From this point of view Anderson localization seems to be relevant for the transition. Whereas the standard single parameter scaling theory predicts no Anderson transition in two dimensions, on the basis of the existing scaling theory of interacting electrons a transition cannot be excluded [6–10]. Besides, several properties of the metallic side, including the low density, i.e., the large value of the electron gas parameter  $r_s$ , the strong increase of the electron  $g$ -factor [11,12], the anomalous magnetoresistance [13,14], and a vanishing compressibility at the critical density [15] can indeed be seen as hints for the relevance of the electron correlations; quantum corrections to the conductivity on the other hand seem to be only small [16–18], at least in the range of temperatures where the main drop of the

resistivity occurs [19].

The main and still open questions are: (1) Is there a real quantum phase transition, or is just a temperature dependent crossover phenomenon observed? (2) What is the nature of the insulating state? (3) Can the metallic phase be described in terms of the standard Fermi-liquid theory?

In this paper we will not touch point one and two. Concerning point three, there is accumulating evidence that the answer is “yes”: at the lowest temperatures and weak magnetic fields standard weak localization physics has been observed in a number of different systems.

In order to obtain a better understanding of the materials, different aspects have to be investigated. We study the influence of spin-orbit coupling on the magnetoconductance.

We assume that the metallic phase can be described in terms of the standard Fermi-liquid theory, and therefore we calculate transport properties in the framework of the Drude-Boltzmann theory. In Si-MOSFET's with low electron density the major spin-orbit term is believed to be due to the lack of inversion symmetry of the confining potential. Originally, there has been the suggestion that the spin-orbit coupling may be responsible for the observed metallic behavior of the resistivity [20]. Although at present such a view is not confirmed by the experiments, it is certainly useful to assess the relevance of the spin-orbit coupling in these systems as well as to understand whether it is related to the puzzling magnetoresistance in a parallel field. In this respect, Chen et al [21] pointed out that such a spin-orbit coupling would induce an anisotropy in the magnetoresistance. The resistivities measured parallel and perpendicular to the in-plane magnetic field are different. Such an anisotropy has been observed in Si-MOSFETs [22].

However, while the original theoretical proposal in Ref. [21] has been formulated in the localized limit, the exper-

imental results have been obtained near and across the MIT. For this reason a direct comparison between theory and experiment is difficult. In a recent paper [23] we have provided a theory valid in the metallic regime. We were able to reproduce correctly a number of the experimental findings. The only drawback of our theory was the wrong sign of the effect, and we speculated that this could be due to the oversimplified assumption of a pure *s*-wave impurity scattering. It is also worth mentioning that anisotropic magnetoresistance has been observed in *GaAs* electron systems [24], and *GaAs* hole systems [25,26]. In these systems, the interpretation is complicated by the intrinsic anisotropy associated with the crystal structure.

In this paper, we study how the form of the microscopic scattering potential affects the anisotropy of the magnetoresistance in the presence of the spin-orbit coupling. In particular, we extend our previous analysis to include the case of small angle scattering. The layout of our paper is the following. In section II we introduce the model and make a first analysis by means of the Boltzmann equation. We adopt the relaxation-time approximation assuming a relaxation rate independent from the position on the Fermi surface. In section III, starting from the Kubo formula we calculate the conductivity within a Green function approach. As a first step, we avoid to specify a microscopic scattering mechanism and we simply introduce, by hand, a lifetime in the one-particle Green function. In so doing we neglect vertex corrections but take into account level broadening and inter-band transitions. As it will be clear in the following, while vertex corrections may give rise to significant changes in the conductivity, the inclusion of level broadening affects only weakly the results. A more sophisticated analysis is carried out in sections IV and V, where we will specify a microscopic mechanism responsible for the finite conductivity, namely elastic scattering. In section IV we will assume *s*-wave scattering. The Green functions and vertex corrections will be calculated in the self-consistent Born approximation. In section V we will explore the consequences of a strongly angle dependent scattering potential. In the limit of strong forward scattering we will find that the sign of the anisotropy is consistent with the experiments. Finally, section VI will contain our conclusions.

## II. THE MODEL AND THE RELAXATION TIME APPROXIMATION

We start from the model Hamiltonian

$$H = \frac{p^2}{2m} + \alpha \boldsymbol{\sigma} \cdot \mathbf{p} \wedge \mathbf{e}_z - \frac{1}{2} g \mu_B \boldsymbol{\sigma} \cdot \mathbf{B} \quad (1)$$

where  $\alpha$  is a parameter describing the spin-orbit coupling due to the confinement field [27],  $\boldsymbol{\sigma}$  is the Pauli matrices

vector, and  $\mathbf{e}_z$  is a unit vector perpendicular to the 2D system. As pointed out recently by Winkler [28], this so-called Rashba model applies for 2D electron systems (like Si-MOS in Ref. [22]), but not for heavy-hole states which are relevant e.g. in Si/SiGe quantum wells. To simplify the notation we introduce the Zeeman energy  $\omega_s = \frac{1}{2} g \mu_B B$  (note that this definition differs by a factor of 2 from the standard one). The *g*-factor in nSi-MOS structures is near two but is growing with decreasing electron density [11]. In the presence of spin-orbit coupling and magnetic field, the original spin degenerate band splits into two bands with energy dispersion

$$E_{\pm}(\mathbf{p}) = p^2/2m \pm \Omega(\mathbf{p}) \quad (2)$$

$$\Omega(\mathbf{p}) = \sqrt{(\alpha p_y - \omega_s)^2 + (\alpha p_x)^2}. \quad (3)$$

We have chosen the direction of the in-plane magnetic field as the  $\mathbf{x}$ -axis. According to the Boltzmann transport theory within the relaxation time approximation, the conductivity tensor at zero temperature is

$$\sigma_{ij} = e^2 \sum_{\mathbf{p}, s} v_s^i v_s^j \tau_{\mathbf{p}, s} \delta(E_s(\mathbf{p}) - \mu), \quad (4)$$

where  $s = \pm$  is the band index and the velocities are  $\mathbf{v}_{\pm} = \nabla_{\mathbf{p}} E_{\pm}(\mathbf{p})$ . By further assuming a constant relaxation rate  $\tau_{\mathbf{p}, s} = \tau_{\text{tr}}$ , the conductivity is proportional to the product of the density of states,  $N_s(\mu)$ , times a Fermi surface average of the Fermi velocities,

$$\sigma_{ij} = e^2 \tau_{\text{tr}} \sum_s N_s(\mu) \langle v_s^i v_s^j \rangle_{FS_s}. \quad (5)$$

We note also that, after integrating by parts Eq.(4), the conductivity may be expressed in terms of the effective mass tensor,

$$\sigma_{ij} = e^2 \tau_{\text{tr}} \sum_{\mathbf{p}, s} \frac{\partial^2 E_s(\mathbf{p})}{\partial p_i \partial p_j} \Theta(\mu - E_s(\mathbf{p})). \quad (6)$$

In the absence of spin-orbit scattering this relation becomes simply  $\sigma = 2e^2 \tau_{\text{tr}} n/m$ , with  $n$  the electron density. We assume that the density does not change with the magnetic field and therefore we have to adjust the chemical potential. As long as both bands are occupied, the chemical potential is nearly constant,  $\mu(\omega_s) \approx \epsilon_F$ . For high fields when the upper band is depopulated it decreases as  $\mu(\omega_s) \approx 2\epsilon_F - \omega_s$ . The chemical potential in the absence of magnetic field is here denoted by  $\epsilon_F$ .

From Eqs.(5) and (6) it is apparent that the transport time drops when we consider the conductivity relative to its value in the absence of magnetic field and spin orbit scattering,  $\sigma_0 = e^2 N_0 v_F^2 \tau_{\text{tr}}$ . For the same reason, the relative anisotropy in the conductivity,  $\Delta\sigma = (\sigma_{xx} - \sigma_{yy})/\sigma_0$ , does not depend on the scattering time  $\tau_{\text{tr}}$  and may be determined from the simple knowledge of the band structure. This observation makes clear the

main goal of our analysis, i.e. to what extent we can understand the small anisotropy in the conductance without making any assumption about the origin of the strong magnetic field dependence of the conductivity itself.

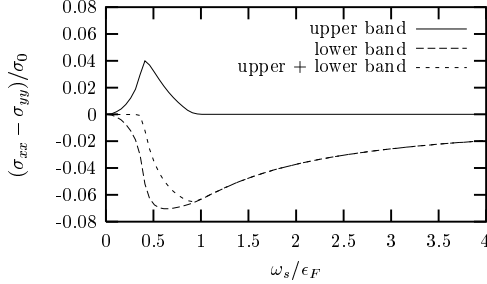


FIG. 1.  $\Delta\sigma$  versus magnetic field ( $\omega_s = g\mu_B B/2$ ) at fixed spin-orbit coupling  $\alpha p_F = 0.4\epsilon_F$  as obtained within the relaxation time approximation with a single scattering rate  $\tau_{tr}$ .

The evaluation of the conductivity via Eq.(5) or (6) is analytically nasty due to the presence of the square root in the energy band dispersion (cf. Eq.(2)). We begin then by presenting the result of the numerical integration of Eq.(6) in Figure 1 which shows  $\Delta\sigma$  for a special value of the spin-orbit term as a function of the magnetic field. We have also plotted the contributions for the two bands separately, and it is seen that at weak magnetic field there is a strong cancellation from the contributions of both bands. At large field the upper band depopulates and therefore does not contribute to the conductivity or its anisotropy.

Some more insight is obtained by considering Eq.(6) in the weak and strong field limits where analytical progress is possible. First we note that  $\Delta\sigma$  must be zero in the limits of very weak and very strong magnetic field, when the Fermi surface becomes rotational symmetric. When  $\omega_s > \alpha p_F$  the dispersion of the two bands is approximately given by

$$E_{\pm}(\mathbf{p}) = p^2/2m \pm (\omega_s - \alpha p_y + (\alpha p_x)^2/2\omega_s), \quad (7)$$

so that the effective mass in the  $x$ -direction, i.e. parallel to the magnetic field, is modified according to

$$\frac{1}{m_{x,\pm}} = \frac{1}{m} \left( 1 \pm \frac{m\alpha^2}{\omega_s} \right). \quad (8)$$

For  $\omega_s > \epsilon_F$ , when only one band is occupied, the anisotropy in the conductivity is thus proportional to  $1/m_x - 1/m$  and explicitly given by

$$\frac{\sigma_{xx} - \sigma_{yy}}{\sigma_0} = -\frac{1}{2} \frac{(\alpha p_F)^2}{\omega_s \epsilon_F}. \quad (9)$$

For  $\omega_s < \epsilon_F$ , when both bands contribute, there is a partial cancellation:

$$\frac{\sigma_{xx} - \sigma_{yy}}{\sigma_0} = -\frac{1}{2} \frac{(\alpha p_F)^2}{\omega_s \epsilon_F} \frac{n_- - n_+}{n} \quad (10)$$

$$\approx -\frac{1}{2} \frac{(\alpha p_F)^2}{\epsilon_F^2}, \quad (11)$$

since the electron densities in the lower and upper band are  $n_{\pm} \approx n(1 \mp \omega_s/\epsilon_F)/2$ .

In order to give the results for the low field limit, we first write (6) explicitly for the given band dispersion

$$\sigma_{xx} - \sigma_{yy} = e^2 \tau_{tr} \alpha^2 \sum_{\mathbf{p}} \frac{(\alpha p_x)^2 - (\omega_s - \alpha p_y)^2}{\Omega^3} \times [\Theta(\mu - E_-(\mathbf{p})) - \Theta(\mu - E_+(\mathbf{p}))]. \quad (12)$$

When  $\Omega \ll \epsilon_F$  one may then approximate the difference of the step functions by a delta function which leads to

$$\frac{\sigma_{xx} - \sigma_{yy}}{\sigma_0} = \frac{1}{2} \frac{(\alpha p_F)^2}{\epsilon_F^2} \times \int_0^{2\pi} \frac{d\theta}{2\pi} \frac{[\alpha p_F \cos(\theta)]^2 - [\omega_s - \alpha p_F \sin(\theta)]^2}{\Omega^2}. \quad (13)$$

Evaluating the integral one arrives at

$$\frac{\sigma_{xx} - \sigma_{yy}}{\sigma_0} = \frac{1}{2} \frac{(\alpha p_F)^2}{\epsilon_F^2} \frac{1 - (\omega_s/\alpha p_F)^2}{(\omega_s/\alpha p_F)^2} \Theta(\omega_s/\alpha p_F - 1). \quad (14)$$

It is interesting to note that (13) is identical to the Fermi surface average of the anomalous part of the velocity  $\mathbf{v}_{\pm} = \mathbf{p}/m \pm \alpha \mathbf{e}_{\mathbf{p}}$ ,

$$\sigma_{xx} - \sigma_{yy} = 2e^2 N_0 \tau_{tr} \alpha^2 \langle (\mathbf{e}_{\mathbf{p}} \cdot \mathbf{e}_x)^2 - (\mathbf{e}_{\mathbf{p}} \cdot \mathbf{e}_y)^2 \rangle_{FS} \quad (15)$$

with  $\mathbf{e}_{\mathbf{p}} = (\alpha \mathbf{p} - \omega_s \mathbf{e}_y)/\Omega$ . At low magnetic field the vector  $\mathbf{e}_{\mathbf{p}}$  makes a full rotation, when averaging over the Fermi surface so that the two dot products averaged over the Fermi surface, in Eq.(15), cancel each other. The anisotropy of the conductivity vanishes. At large field  $\mathbf{e}_{\mathbf{p}}$  becomes locked in  $y$ -direction. The conductivity becomes then anisotropic at a magnetic field value  $\omega_s = \alpha p_F$ . Fig.2 shows the numerically determined anisotropy for different strengths of the spin-orbit coupling. The edge behavior at  $\alpha p_F = \omega_s$  predicted by Eq.(14) is clearly visible.

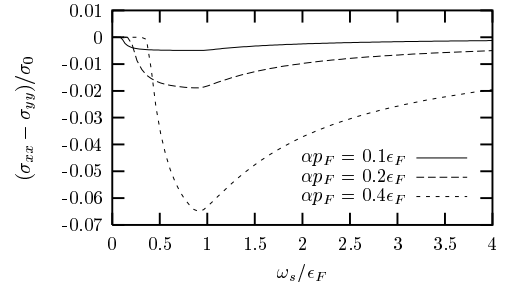


FIG. 2.  $\Delta\sigma$  versus magnetic field as obtained within the relaxation time approximation for various strengths of the spin-orbit coupling.

When  $\epsilon_F > \omega_s \gg \alpha p_F$  the anisotropy is nearly constant, which agrees both with our weak and strong field expansion.

### III. THE CONDUCTIVITY WITHIN THE KUBO FORMULA APPROACH

In this section we go beyond the Boltzmann equation approach in the relaxation-time approximation and calculate the conductivity via the Kubo formula. The starting point is the response kernel  $Q_{ij}$  which at zero temperature is given by

$$Q_{ij}(q) = ie^2 \sum_{\mathbf{p}} \int_{-\infty}^{\infty} \frac{d\epsilon}{2\pi} \text{Tr} [j^i(p, q) G(p_+) J^j(p, q) G(p_-)] - \frac{e^2 N}{m} \delta_{ij}. \quad (16)$$

In the above we are using four vectors  $p = (\epsilon, \mathbf{p})$  and  $q = (\omega, \mathbf{q})$  with  $p_{\pm} = p \pm q/2$ ; the trace is over the spin. In the presence of the spin-orbit coupling the bare current vertex differs from the standard expression and is given by

$$\mathbf{j} = \frac{\mathbf{p}}{m} - \alpha \sigma \wedge \mathbf{e}_z. \quad (17)$$

The evaluation of the dressed vertex will be considered in section IV. The conductivity tensor is obtained by considering the limit

$$\sigma_{ij} = \lim_{\omega \rightarrow 0} \frac{Q_{ij}(\omega, 0)}{i\omega}. \quad (18)$$

By splitting the energy integration into regions where the Green functions have defined analytical properties, one may separate the kernel into two parts. In the first both the Green functions are retarded or advanced. This part cancels exactly the diamagnetic term, i.e.,

$$i \sum_{\mathbf{p}} \int_{-\infty}^{\infty} \frac{d\epsilon}{2\pi} \text{Tr} [j^i(p) G(p) J^j(p) G(p)] - \frac{N}{m} \delta_{ij} = 0. \quad (19)$$

The cancellation is made explicit in appendix A by exploiting the Ward identity due to the gauge invariance. The second term is given by

$$\begin{aligned} \sigma_{ij} = \frac{e^2}{4\pi} \sum_{\mathbf{p}} \text{Tr} & \left[ 2j^i(p) G^R(p) J_{RA}^j(p) G^A(p) \right. \\ & - j^i(p) G^R(p) J_{RR}^j(p) G^R(p) \\ & \left. - j^i(p) G^A(p) J_{AA}^j(p) G^A(p) \right]. \end{aligned} \quad (20)$$

The dressed vertex depends whether it is connected to a pair of retarded and advanced Green functions or a pair of Green functions with equal analytic properties.

In order to make contact with the analysis of the previous section, we temporarily make no assumption regarding a specific scattering mechanism and simply take a (retarded) Green function of the form

$$(G_{\pm}^R)^{-1}(\mathbf{p}, \epsilon) = \epsilon - E_{\pm}(\mathbf{p}) + \mu + i/2\tau, \quad (21)$$

where the scattering time  $\tau$  is of some unknown origin. Let us also neglect the vertex corrections, i.e.  $J \rightarrow j$ . We are aware that neglecting vertex corrections often leads to serious errors in the calculation of the conductivity, but their calculation requires a specific scattering mechanism. The conductivity is then given by

$$\sigma_{ij} = \frac{e^2}{\pi} \sum_{\mathbf{p}} \sum_{a,b=\pm} \langle a | j^i(p) | b \rangle \text{Im}(G_b^R(\mathbf{p})) \langle b | j^j(p) | a \rangle \text{Im}(G_a^R(\mathbf{p})). \quad (22)$$

In the limit of weak scattering  $1/\tau \rightarrow 0$ ,  $\text{Im}G^R$  becomes strongly peaked at the Fermi energy. As a result intra-band contributions ( $a = b$ ) dominate in this limit. Neglecting then the inter-band terms ( $a \neq b$ ) and with the approximation

$$\text{Im}G_a^R \text{Im}G_a^R \approx \tau \pi \delta(\epsilon - E_a + \mu) \quad (23)$$

one recovers the expression for the conductivity of the Boltzmann equation approach, when we identify  $\tau_{\text{tr}}$  with  $\tau$ . In the general case with a finite scattering rate, the inter-band terms and deviations of  $\text{Im}G^R \text{Im}G^R$  from the delta function have to be taken into account. This is clearly demonstrated in Fig.3.

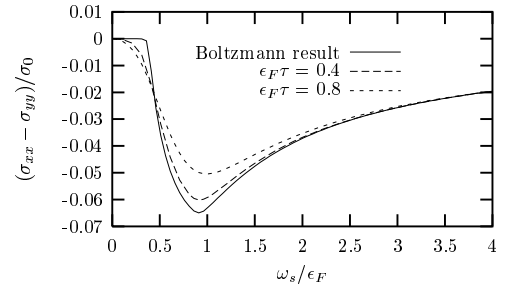


FIG. 3.  $\Delta\sigma$  versus magnetic field for  $\alpha p_F = 0.4$  and various scattering strengths. Scattering events are taken into account in the broadening of the energy levels as discussed in the text.

Taking into account a finite  $1/\tau$  the sharp edge of the anisotropy at  $\omega_s = \alpha p_F$  disappears, although the anisotropy curves do not change much even in the strong scattering case where  $\epsilon_F \tau = 0.8$ .

Going beyond this crude approximation in calculating the conductivity we have to pay the price to make an assumption on the scattering mechanism at play. We assume elastic scattering, and we neglect quantum interference corrections to the conductivity. In the following we will first calculate the conductivity in the case of a

pure s-wave scattering. The results will be obtained in the framework of the self-consistent Born approximation. Then we will allow an arbitrary  $p$ -dependence of the scattering potential. In that case we will confine ourselves to the weak disorder limit.

#### IV. S-WAVE SCATTERING

In this section we consider a specific microscopic origin for the conductivity, namely elastic scattering. For simplicity we assume a impurity potential with short range Gaussian correlations

$$\langle U(\mathbf{x})U(\mathbf{x}') \rangle = \frac{1}{2\pi N_0 \tau} \delta(\mathbf{x} - \mathbf{x}'). \quad (24)$$

We will calculate the conductivity in the framework of the self-consistent Born approximation, including the corresponding vertex corrections.

The self-energy is then given by

$$\Sigma = \frac{1}{2\pi N_0 \tau} \sum_{\mathbf{p}} G(p). \quad (25)$$

To deal with the above matrix equation we expand it in Pauli matrices. The Green function can be written as  $G = G_0 \sigma_0 + G_1 \sigma_1 + G_2 \sigma_2$  with

$$\begin{aligned} G_0 &= \frac{1}{2} [G_+ + G_-] \\ G_1 &= -\frac{\omega_s - \alpha p_y - \Sigma_1}{2\Omega} [G_+ - G_-] \\ G_2 &= -\frac{\alpha p_x}{2\Omega} [G_+ - G_-], \end{aligned} \quad (26)$$

where  $\Omega(\mathbf{p}) = \sqrt{(\alpha p_y - \omega_s + \Sigma_1)^2 + \alpha^2 p_x^2}$  and

$$G_{\pm} = (\epsilon - p^2/2m + \mu \mp \Omega - \Sigma_0)^{-1}. \quad (27)$$

Because the self-energy shares the matrix structure of the Green function, it has no  $\sigma_3$  component. Furthermore it turns out that  $\Sigma_2 = 0$  always solves the self-consistency equation, due to the symmetry  $p_x \rightarrow -p_x$ . As a result the self-energy has the form  $\Sigma_0 \sigma_0 + \Sigma_1 \sigma_1$ . To appreciate the meaning of the two self-energy components, we briefly consider the case with no spin-orbit coupling. This is especially important for understanding the behavior at large magnetic field. The real part of the self energy  $\Sigma_0$  shifts the energy spectrum by a constant. Since we have to adjust the chemical potential in order to keep the particle number fixed,  $\text{Re}\Sigma_0$  can be safely neglected. The real part of  $\Sigma_1$  may be re-absorbed into a renormalization of the Zeeman energy. We then concentrate on the imaginary part, and find

$$\text{Im}\Sigma^R = -\left(\frac{1}{2\tau_0}\sigma_0 + \frac{1}{2\tau_1}\sigma_1\right) \quad (28)$$

with

$$\frac{1}{\tau_0} \approx \frac{1}{\tau} \frac{N_+ + N_-}{2N_0} \quad (29)$$

$$\frac{1}{\tau_1} \approx \frac{1}{\tau} \frac{N_- - N_+}{2N_0}. \quad (30)$$

The sum or difference  $1/\tau_{\mp} = 1/\tau_0 \pm 1/\tau_1$  are nothing but the scattering times for the two spin subbands. For weak magnetic field ( $\omega_s < \epsilon_F$ ), the density of states in the two subbands are identical and therefore  $1/\tau_{\pm} = 1/\tau_0 = 1/\tau$ . In the strong field limit ( $\omega_s > \epsilon_F$ ) the upper band is depopulated, so that  $1/\tau_1 = 1/\tau_0 = 1/2\tau$ . The scattering rate in the empty band is zero due to the vanishing density of states. Typical numerical results are shown in Fig.4. Although the general shape of the curves is as discussed above, it is seen that for the disorder strengths we consider there are already considerable modifications.

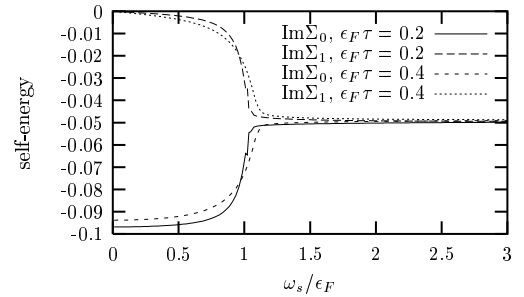


FIG. 4. The imaginary part of the self-energy for  $\alpha p_F = 0.4$  and  $\epsilon_F \tau = 0.2, 0.4$  as a function of the magnetic field. The numbers for  $\epsilon_F \tau = 0.4$  have been divided by two.

#### A. The vertex corrections

We now move to consider vertex corrections, following the standard approach in the literature (see for example [29]). Physically vertex corrections are important for obtaining the correct momentum relaxation time, which generally differs from the quasi-particle lifetime. For the choice of a pure s-wave scattering potential, as in Eq.(24), in the absence of spin-orbit coupling, the momentum relaxation time coincides with the quasi-particle lifetime. This corresponds, diagrammatically, to the fact that there is no dressing of the current vertex with momentum independent impurity lines. In the presence of spin-orbit coupling this is no longer the case due to the presence of extra terms in the current vertex of Eq.(17). The dressed current vertex is obtained by solving the equation

$$J_{RA}^{x,y} = j^{x,y} + \frac{1}{2\pi N_0 \tau} \sum_{\mathbf{p}} G^R J_{RA}^{x,y} G^A. \quad (31)$$

A similar equation exists for the other energy ranges when one has a pair of retarded or advanced Green functions. The strategy to solve the equation is to separate momentum dependent from momentum independent

parts, expand the spin-dependent quantities in the Pauli matrix basis, and finally invert the resulting matrix equations.

We begin by separating the  $p$ -dependent and the  $p$ -independent parts of the current operator:

$$j^{x,y} = p_{x,y}/m \mp \alpha \sigma_{2,1} \quad (32)$$

$$J^{x,y} = J_0^{x,y}(p) + \Gamma^{x,y}. \quad (33)$$

Since we consider a  $p$ -independent impurity scattering the  $J_0^{x,y}(p)$  part is not dressed, i.e.,

$$J_0^{x,y}(p) = p_{x,y}/m. \quad (34)$$

The equation for the momentum independent part of the current vertex reads

$$\Gamma_{ss'}^{x,y} = \gamma_{ss'}^{x,y} + \frac{1}{2\pi N_0 \tau} \sum_{\mathbf{p}} \sum_{ab} G_{sa}^R \Gamma_{ab}^{x,y} G_{bs'}^A. \quad (35)$$

We included here the spin indices  $s, s', a$ , and  $b = \uparrow, \downarrow$ . The quantities  $\gamma^{x,y}$  are a sum of the bare vertices  $\mp \alpha \sigma_{2,1}$  and a term which is generated by  $p_{x,y}/m$ ,

$$\gamma_{ss'}^{x,y} = \mp \alpha (\sigma_{2,1})_{ss'} + \frac{1}{2\pi N_0 \tau} \sum_{\mathbf{p}} \sum_a \frac{p_{x,y}}{m} G_{sa}^R G_{as'}^A. \quad (36)$$

In the Pauli matrix space the vertex equation becomes:

$$\Gamma_{\rho}^i = \gamma_{\rho}^i + \frac{1}{2} \sum_{\mu\nu\lambda} I_{\mu\nu} \text{Tr}(\sigma_{\rho} \sigma_{\mu} \sigma_{\lambda} \sigma_{\nu}) \Gamma_{\lambda}^i \quad (37)$$

with

$$I_{\mu\nu} = \frac{1}{2\pi N_0 \tau} \sum_{\mathbf{p}} G_{\mu}^R G_{\nu}^A. \quad (38)$$

Some of the integrals  $I_{\mu\nu}$  are zero and so the equations simplify. The final result is

$$\begin{pmatrix} \Gamma_0^y \\ \Gamma_1^y \end{pmatrix} = \begin{pmatrix} \gamma_0^y \\ \gamma_1^y \end{pmatrix} + \begin{pmatrix} I_{00} + I_{11} + I_{22} & I_{01} + I_{10} \\ I_{01} + I_{10} & I_{00} + I_{11} - I_{22} \end{pmatrix} \begin{pmatrix} \Gamma_0^y \\ \Gamma_1^y \end{pmatrix} \quad (39)$$

$$\begin{pmatrix} \Gamma_2^x \\ \Gamma_3^x \end{pmatrix} = \begin{pmatrix} \gamma_2^x \\ 0 \end{pmatrix} + \begin{pmatrix} I_{00} - I_{11} + I_{22} & i(I_{01} - I_{10}) \\ -i(I_{01} - I_{10}) & I_{00} - I_{11} + I_{22} \end{pmatrix} \begin{pmatrix} \Gamma_2^x \\ \Gamma_3^x \end{pmatrix}, \quad (40)$$

where the bare vertices  $\gamma^{x,y}$  are

$$\begin{aligned} \gamma_0^y &= J_{00}^y + J_{11}^y + J_{22}^y \\ \gamma_1^y &= \alpha + J_{01}^y + J_{10}^y \\ \gamma_2^x &= -\alpha + J_{02}^x + J_{20}^x \end{aligned} \quad (41)$$

with

$$J_{\mu\nu}^i = \frac{1}{2\pi N_0 \tau} \sum_{\mathbf{p}} G_{\mu}^R(p_i/m) G_{\nu}^A. \quad (42)$$

One might try to determine the dressed vertices  $\Gamma_{\rho}^{x,y}$  by solving the above matrix equations. Whereas this is straightforward for  $\Gamma_{2,3}^x$ , the equation for  $\Gamma_{0,1}^y$  needs special care. The analysis of Eq.(39) shows that the matrix on the right-hand side of (39) has an eigenvalue equal to one. As a consequence the matrix

$$\begin{pmatrix} 1 - (I_{00} + I_{11} + I_{22}) & -(I_{01} + I_{10}) \\ -(I_{01} + I_{10}) & 1 - (I_{00} + I_{11} - I_{22}) \end{pmatrix}$$

cannot be inverted, and (39) has no unique solution. This property follows from charge conservation and manifests in the charge density vertex being singular in the low frequency, long wavelength limit (see also App.A). To see explicitly this property consider the imaginary part of the self-energy:

$$\begin{aligned} \Sigma^R - \Sigma^A &= \frac{1}{2\pi N_0 \tau} \sum_{\mathbf{p}} (G^R - G^A) \\ &= \frac{1}{2\pi N_0 \tau} \sum_{\mathbf{p}} G^R (\Sigma^R - \Sigma^A) G^A. \end{aligned} \quad (43)$$

By means of Eq.(43) we can relate the imaginary part of the self-energy with the integrals over pairs of retarded and advanced Green functions  $I_{\mu\nu}$ . Expanding in Pauli matrices we find

$$(\Sigma^R - \Sigma^A)_{\rho} = \frac{1}{2} \text{Tr}(\sigma^{\rho} \sigma^{\mu} \sigma^{\lambda} \sigma^{\nu}) I_{\mu\nu} (\Sigma^R - \Sigma^A)_{\lambda} \quad (44)$$

which gives rise to the equation

$$\begin{pmatrix} 1/\tau_0 \\ 1/\tau_1 \end{pmatrix} = \begin{pmatrix} I_{00} + I_{11} + I_{22} & I_{01} + I_{10} \\ I_{01} + I_{10} & I_{00} + I_{11} - I_{22} \end{pmatrix} \begin{pmatrix} 1/\tau_0 \\ 1/\tau_1 \end{pmatrix}. \quad (45)$$

This means that the vector of the scattering rates is an eigenvector of the above matrix with eigenvalue  $\lambda_0 = 1$ . The second eigenvalue is then given by  $\lambda_1 = 2I_{00} + 2I_{11} - 1$ . We now demonstrate that the eigenvector corresponding to  $\lambda_1$  is proportional to  $(\gamma_0^y, \gamma_1^y)$ . We start from

$$\frac{1}{2\pi N_0 \tau} \text{Tr} \sum_{\mathbf{p}} j^y (G^R - G^A) = 0. \quad (46)$$

We use again the relation  $G^R - G^A = G^R (\Sigma^R - \Sigma^A) G^A$  and arrive at

$$\frac{1}{4\pi N_0 \tau} \sum_{\mathbf{p}} \frac{p^y}{m} \text{Tr} \left[ \sigma^{\mu} \left( \frac{1}{\tau_0} \sigma^0 + \frac{1}{\tau_1} \sigma^1 \right) \sigma^{\nu} \right] G_{\mu}^R G_{\nu}^A + \frac{\alpha}{\tau_1} = 0 \quad (47)$$

with the final result that

$$\frac{1}{\tau_0} (J_{00}^y + J_{11}^y + J_{22}^y) + \frac{1}{\tau_1} (\alpha + J_{01}^y + J_{10}^y) = 0, \quad (48)$$

so that the vector  $(\gamma_0^y, \gamma_1^y)$  is perpendicular to  $(1/\tau_0, 1/\tau_1)$  and therefore necessarily is the second eigenvector of the matrix on the right hand side of (45). The solutions of (45) for the dressed vertex  $(\Gamma_0^y, \Gamma_1^y)$  are then given by  $(\Gamma_0^y, \Gamma_1^y) = (\gamma_0^y, \gamma_1^y)/(1 - \lambda_1)$  plus an arbitrary vector proportional to  $(1/\tau_0, 1/\tau_1)$ . From (46) and (47) one observes that this arbitrary vector is irrelevant for the conductivity. For simplicity we choose it to be zero.

Numerical results for the dressed vertices are shown in the figure. Notice that Eqs.(45) and (48) provide a nontrivial consistency check for the numerics.

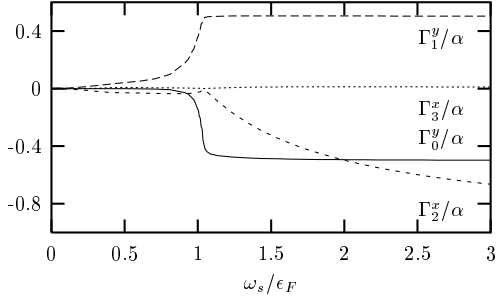


FIG. 5. The dressed vertices  $\Gamma_0 \dots \Gamma_3$  in units of  $\alpha$  as a function of the magnetic field. Here we chose  $\alpha p_F = 0.4\epsilon_F$  and  $1/(\epsilon_F\tau) = 0.2$ . Remember that the bare vertices are  $\gamma_0^y = \gamma_3^x = 0$  and  $\gamma_1^y = -\gamma_2^x = \alpha$ ; the asymptotic values in the strong field limit are  $\Gamma_1^y = -\Gamma_0^y = \alpha/2$ ,  $\Gamma_2^x = -\alpha$ , and  $\Gamma_3^x = 0$ . Notice that  $\Gamma_2^x$  reaches the asymptotic value for high magnetic field only very slowly.

It is seen that the anomalous part of the current operator is strongly affected by the vertex corrections. In particular for weak magnetic field the quantities  $\Gamma_\mu$  become extremely small, so that the anomalous part of the current operator is canceled,  $J^i \approx p^i/m$ . In the limits  $\epsilon_F\tau \ll 1$  and  $\omega_s = 0$  this cancellation is exact as we now show. When  $\omega_s = 0$  the Green functions are

$$\begin{aligned} G_0^{R(A)} &= \frac{1}{2} [G_+^{R(A)} + G_-^{R(A)}] \\ G_1^{R(A)} &= \frac{\sin(\theta)}{2} [G_+^{R(A)} - G_-^{R(A)}] \\ G_2^{R(A)} &= -\frac{\cos(\theta)}{2} [G_+^{R(A)} - G_-^{R(A)}], \end{aligned} \quad (49)$$

where

$$G_\pm^{R(A)} = (\epsilon - p^2/2m \mp \alpha p \pm i/2\tau)^{-1}. \quad (50)$$

The first step is to evaluate the effective bare vertices entering the expression for the conductivity, i.e.,  $\gamma^i$ . This can be done by evaluating the integrals we denoted by  $J_{\mu\nu}^i$ . Because the Green function in the case  $\omega_s = 0$  has a simple angular dependence, one may directly conclude that the integrals  $J_{00}$ ,  $J_{11}$ , and  $J_{22}$  are zero. With the approximation  $G_\pm^R G_\pm^A \approx 2\pi\tau\delta(\epsilon - E_\pm)$  the remaining integrals are readily found to be  $J_{01} + J_{10} = -\alpha$  and  $J_{02} + J_{20} = \alpha$  with the result that the vertices  $\gamma^i$  and consequently the dressed vertices  $\Gamma_\mu$  are zero.

In the strong field limit  $\omega_s \rightarrow \infty$  we find  $J_x = p_x/m - \alpha\sigma_2$ ,  $J_y = p_y/m + \alpha(\sigma_1 - \sigma_0)/2$ , compare Fig.5. Thus for  $J_x$  the vertex corrections are absent but they seem to be present for  $J_y$ . On the other hand as we noted before the solution of the vertex equation is not unique and also  $J_y = p_y/m + \alpha\sigma_1$  solves (31), i.e. there are no vertex corrections to the conductivity. We will discuss the strong field limit in more detail in the next subsection.

## B. The conductivity

Having discussed the vertex corrections we can now consider their effect on the conductivity. We do not find a strong magnetoresistance, compare also Fig.8 below. Typical numerical results for the anisotropy in the conductivity are shown in Fig.6. The most striking features are the change of sign at low magnetic fields and the sharp structure around  $\omega_s = \epsilon_F$ .

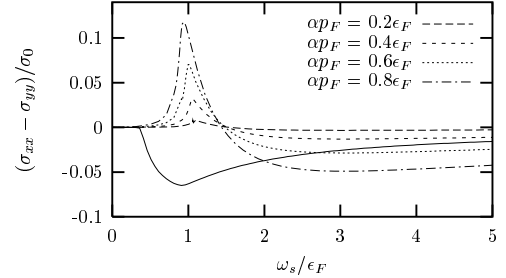


FIG. 6. Anisotropy in the magneto-conductance for  $s$ -wave impurity scattering,  $1/(\epsilon_F\tau) = 0.2$  and various spin-orbit energies. For comparison we included the results of the relaxation time approximation ( $\alpha p_F = 0.4\epsilon_F$ ; full line). For not too strong fields, the vertex corrections change the sign of the effect.

In Fig.7 it is seen that the structure around  $\omega_s \approx \epsilon_F$  becomes more pronounced the less disordered the system becomes. For  $\epsilon_F\tau \ll 1$  a step in the anisotropy evolves at that energy. The step is related to the van-Hove singularity in the density of states at the band edge of the upper band. Disorder smears out this singularity.

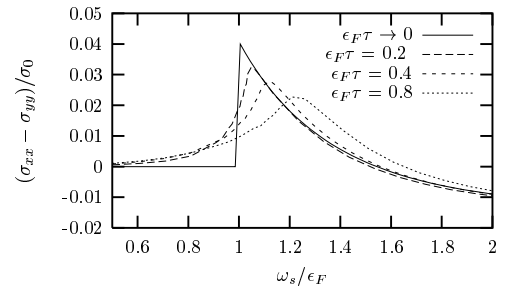


FIG. 7. Anisotropy in the magneto-conductance for  $\alpha p_F = 0.4$  and varying the disorder. The curve in the limit of weak disorder was obtained within the approximation described in the section on small angle scattering.

In order to have an understanding of these effects we will calculate the conductivity analytically for strong magnetic fields. The limit  $\omega_s \rightarrow \infty$  is understood easily. There is just one band occupied with the dispersion given by  $E_-(\mathbf{p}) = p^2/2m - \omega_s + \alpha p^y$ . The Fermi surface is a circle which is centered around  $(0, -m\alpha)$ . Shifting  $p^y$  to  $p'^y = p^y + m\alpha$  the problem becomes rotational symmetric. The (bare) current operator in the lower band is then simply of the standard form  $j^{x,y} = p'^{x,y}/m$ . As a consequence the  $p$ -independent disorder potential does not renormalize the current operator, and the conductivity is  $\sigma_{xx} = \sigma_{yy} = \sigma_0$ . In particular there is no anisotropy in the conductance.

Lowering the magnetic field various contributions to the anisotropy appear. Expanding the square roots in the energy dispersion, the Green functions for the two subbands read

$$G_{\pm}^R(\omega, \mathbf{p}) = \left( \omega + \mu \mp \omega_s - \frac{p_x^2}{2m_{\pm}} - \frac{p_y^2}{2m} \pm \alpha p_y + i \frac{1}{2\tau_{\pm}} \right)^{-1} \quad (51)$$

where

$$m_{\pm} = m \left( 1 \pm \frac{m\alpha^2}{\omega_s} \right)^{-1} \quad (52)$$

$$\frac{1}{\tau_{\pm}} = \frac{1}{\tau_0} \mp \frac{1}{\tau_1} \left( 1 - \frac{1}{2} \frac{\alpha^2 p_x^2}{\omega_s^2} \right). \quad (53)$$

We discussed the effective mass anisotropy already in the framework of the relaxation time approximation. Allowing the scattering times in the two bands to be different, the result of section II is generalized to

$$\left( \frac{\sigma_{xx} - \sigma_{yy}}{\sigma_0} \right)_{\text{mass}} = -\frac{1}{2} \frac{(\alpha p_F)^2}{\omega_s \epsilon_F} \frac{\tau_- n_- - \tau_+ n_+}{\tau_- n_- + \tau_+ n_+}. \quad (54)$$

Further contributions to  $\Delta\sigma$  are due to the anisotropic relaxation rate. The scattering times  $\tau_0$  and  $\tau_1$  must be obtained by solving the self-consistent Born approximation. In the weak disorder limit the van-Hove singularity at the band edge of the upper band leads to a singular (=step) behavior of the two scattering rates. Such singular behavior is smeared out when disorder becomes stronger (compare Fig.4). For simplicity we restrict the following discussion to the weak disorder case. The angular dependent rate which we obtained by expanding the square root in the energy dispersion may also be obtained by considering the scattering probability in the eigenstate basis. The latter can be written as

$$W_{\mathbf{p}\mathbf{p}'}^{\text{eff}} = |U|^2 \frac{1}{2} \begin{pmatrix} 1 + \mathbf{e}_{\mathbf{p}} \cdot \mathbf{e}_{\mathbf{p}'} & 1 - \mathbf{e}_{\mathbf{p}} \cdot \mathbf{e}_{\mathbf{p}'} \\ 1 - \mathbf{e}_{\mathbf{p}} \cdot \mathbf{e}_{\mathbf{p}'} & 1 + \mathbf{e}_{\mathbf{p}} \cdot \mathbf{e}_{\mathbf{p}'} \end{pmatrix}. \quad (55)$$

The vector  $\mathbf{e}_{\mathbf{p}}$  has been defined below Eq.(15). In the high field limit

$$W_{\mathbf{p}\mathbf{p}'}^{\text{eff}} = |U|^2 \begin{pmatrix} 1 & 0 \\ 0 & 1 \end{pmatrix} - |U|^2 \frac{1}{4} \frac{\alpha^2 (p_x - p'_x)^2}{\omega_s^2} \begin{pmatrix} 1 & -1 \\ -1 & 1 \end{pmatrix}, \quad (56)$$

i.e. the effective scattering probability is anisotropic. The anisotropy in the scattering rate is due to the term proportional to  $(\alpha p_x)^2/\omega_s^2$  and is found as  $\delta(1/\tau_{\pm}) = \mp 2\pi |U|^2 (\alpha p_x/2\omega_s)^2 (N_+ - N_-)$ . For  $\omega_s < \epsilon_F$  the two density of states are practically identical, so  $1/\tau_{\pm}$  remains isotropic. Only for  $\omega_s > \epsilon_F$  the scattering rate is anisotropic and is a source for the anisotropy in the conductivity, which we determine as

$$\left( \frac{\sigma_{xx} - \sigma_{yy}}{\sigma_0} \right)_{\tau_-} = \frac{1}{4} \frac{(\alpha p_F)^2}{\omega_s^2}. \quad (57)$$

We now consider the vertex corrections. To leading order in  $1/\omega_s$  we need to calculate only the diagram with one impurity line. It is of the type

$$\delta\sigma_{ii} = \frac{e^2}{2\pi} \sum_{\mathbf{p}, \mathbf{p}'} j^i(\mathbf{p}) G_{\mathbf{p}}^R G_{\mathbf{p}}^A W_{\mathbf{p}\mathbf{p}'}^{\text{eff}} G_{\mathbf{p}'}^R G_{\mathbf{p}'}^A j^i(\mathbf{p}'), \quad (58)$$

which one has to sum over the two bands. Because the scattering probability depends in the strong magnetic field limit only on the  $x$  component of the momentum, only  $\sigma_{xx}$  is affected. We find by evaluating Eq.(58)

$$\left( \frac{\sigma_{xx} - \sigma_{yy}}{\sigma_0} \right)_{\text{vertex}} = \frac{1}{2} \frac{(\alpha p_F)^2}{\omega_s^2} \left( \frac{n_+ - n_-}{n} \right)^2. \quad (59)$$

When  $\omega_s < \epsilon_F$  the vertex correction cancels with the contribution due to the mass anisotropy since  $(n_+ - n_-)/n \approx \omega_s/\epsilon_F$ , so that the anisotropy vanishes. In the case  $\omega_s > \epsilon_F$  the sum of the three terms we discussed gives

$$\Delta\sigma/\sigma_0 = -\frac{1}{2} \frac{(\alpha p_F)^2}{\omega_s \epsilon_F} + \frac{3}{4} \frac{(\alpha p_F)^2}{\omega_s^2} \quad (60)$$

in full agreement with the numerical results of Fig.(6).

We conclude this section by noting that the order of magnitude of the anisotropy in the microscopic calculation is the same as in the relaxation-time approximation. Here however also the transport time becomes anisotropic. The competition with the mass anisotropy kills  $\Delta\sigma$  when  $\omega_s < \epsilon_F$ . In the next section we will see that this cancellation is a peculiar consequence of the momentum independent impurity scattering.

## V. SMALL ANGLE SCATTERING

We will now drop the assumption of a  $p$ -independent impurity potential and consider the more general case. For simplicity we will restrict ourselves to the weak disorder limit, where we will neglect the disorder broadening



of the energy levels, and terms which are related to the off-diagonal matrix elements of the current operator (in the eigenstate basis). The results obtained within these approximations are fully equivalent with the Boltzmann equation approach, as it is discussed in Appendix B. In the energy state eigenbasis the dressing equation for the current vertex then reads

$$J_{\mathbf{p}m}^{x,y} = j_{\mathbf{p}m}^{x,y} + \sum_{\mathbf{p}'m'} W_{\mathbf{p}m;\mathbf{p}'m'}^{\text{eff}} G_{\mathbf{p}'m'}^R G_{\mathbf{p}'m'}^A J_{\mathbf{p}'m'}^{x,y}, \quad (61)$$

with

$$G_{\mathbf{p}m}^R G_{\mathbf{p}m}^A \approx 2\pi\tau_{\mathbf{p}m}\delta(\mu - E_m(\mathbf{p})). \quad (62)$$

The lifetime is determined from the expression

$$1/\tau_{\mathbf{p}m} = 2\pi \sum_{\mathbf{p}'m'} W_{\mathbf{p}m;\mathbf{p}'m'}^{\text{eff}} \delta(\mu - E_{m'}(\mathbf{p}')). \quad (63)$$

We determine the dressed current operator with an expansion in eigenfunctions, following Ref. [30]: let  $\phi_{\mathbf{p}m}^l$  be the full set of eigenfunctions of the operator

$$\sum_{\mathbf{p}'m'} W_{\mathbf{p}m;\mathbf{p}'m'}^{\text{eff}} G_{\mathbf{p}'m'}^R G_{\mathbf{p}'m'}^A \phi_{\mathbf{p}'m'}^l = \lambda^l \phi_{\mathbf{p}m}^l, \quad (64)$$

which are normalized according to

$$\sum_{\mathbf{p}m} \phi_{\mathbf{p}m}^l G_{\mathbf{p}m}^R G_{\mathbf{p}m}^A \phi_{\mathbf{p}m}^{l'} = \delta_{ll'}. \quad (65)$$

The kernel entering the integral equation (61) may be expanded as

$$W_{\mathbf{p}m;\mathbf{p}'m'}^{\text{eff}} = \sum_l \lambda_l \phi_{\mathbf{p}m}^l \phi_{\mathbf{p}'m'}^l. \quad (66)$$

One further notices that  $1/\tau_{\mathbf{p}m}$  is an eigenfunction with eigenvalue one,  $\lambda^0 = 1$  and  $\phi_{\mathbf{p}m}^0 \propto 1/\tau_{\mathbf{p}m}$ . Furthermore the bare current operator is perpendicular to this eigenfunction. This can be shown in analogy with the discussion developed in the case of *s*-wave scattering in section IV.A. With the expansion

$$j_{\mathbf{p}m}^{x,y} = \sum_l j_l^{x,y} \phi_{\mathbf{p}m}^l; \quad j_l^{x,y} = \sum_{\mathbf{p}m} j_{\mathbf{p}m}^{x,y} G_{\mathbf{p}m}^R G_{\mathbf{p}m}^A \phi_{\mathbf{p}m}^l. \quad (67)$$

the dressed current operator can be expressed as

$$J_{\mathbf{p}m}^{x,y} = \sum_{l \neq 0} \phi_{\mathbf{p}m}^l \frac{1}{1 - \lambda_l} j_l^{x,y}, \quad (68)$$

from which we finally obtain the conductivity by inserting it in Eq.(20). Before showing the results for the anisotropy and analyzing the vertex corrections in the presence of small angle scattering, it is instructive to consider the zero magnetic field case first. As discussed in section IV for the case of *s*-wave scattering, the vertex corrections have their most dramatic effect on the

anisotropy in the limit of weak magnetic field. In the zero magnetic field limit, the structure of the dressed current vertex simplifies considerably. The scattering probability  $W_{\mathbf{p}\mathbf{p}'}$  and the effective scattering probability become isotropic, i.e. they depend only on the angle between  $\mathbf{p}$  and  $\mathbf{p}'$ . One can then expand

$$W^{\text{eff}} = W^0 + 2W^1 \cos(\theta - \theta') + \dots, \quad (69)$$

where  $W^{\text{eff}}$ ,  $W^0$ , and  $W^1$  have still the two by two matrix structure. The lifetimes and the dressed current operator are expressed as

$$1/\tau_+ = 2\pi N_+ W_{++}^0 + 2\pi N_- W_{+-}^0 \quad (70)$$

$$1/\tau_- = 2\pi N_+ W_{-+}^0 + 2\pi N_- W_{--}^0 \quad (71)$$

and

$$\begin{pmatrix} J_+^{x,y} \\ J_-^{x,y} \end{pmatrix} = \begin{pmatrix} j_+^{x,y} \\ j_-^{x,y} \end{pmatrix} + \begin{pmatrix} 2\pi N_+ \tau_+ W_{++}^1 & 2\pi N_- \tau_- W_{+-}^1 \\ 2\pi N_+ \tau_+ W_{-+}^1 & 2\pi N_- \tau_- W_{--}^1 \end{pmatrix} \begin{pmatrix} J_+^{x,y} \\ J_-^{x,y} \end{pmatrix} \quad (72)$$

where  $N_{\pm}(\epsilon) = N_0(1 \mp m\alpha/\sqrt{(m\alpha)^2 + 2m\epsilon})$  and  $\mathbf{j}_{\pm} = \nabla_{\mathbf{p}} E_{\pm}(\mathbf{p})$  are the density of states and the bare current vertices in the two bands. For short range impurity potential, from Eq.(55), one finds  $W_{++}^0 = \dots = 1/4\pi N_0\tau$ ,  $\tau_{\pm} = \tau$ , and  $W_{++}^1 = -W_{+-}^1 = \dots = 1/8\pi N_0\tau$ . Going through the algebra one may verify our earlier result that the vertex corrections cancel the anomalous velocity operator in this limit,  $\mathbf{J}_{\pm} = \mathbf{p}_{\pm}/m$ . Generally however this is not the case. In the extreme forward scattering limit in particular, one can neglect the off-diagonal terms  $W_{+-}^1$  and arrives at the standard expression for single, isotropic bands  $\mathbf{J}_{\pm} = \mathbf{j}_{\pm}\tau_{\text{tr}}/\tau$  with  $1/\tau_{\text{tr}} = N_{\pm} \int d\theta W_{\pm\pm}^{\text{eff}}(\theta)[1 - \cos(\theta)]$ .

Let us now consider a Gaussian scattering probability,

$$W_{\mathbf{p}\mathbf{p}'} = W \exp(-r_0^2(\mathbf{p} - \mathbf{p}')^2/2). \quad (73)$$

The electron spin is assumed to be conserved, so this scattering potential has still to be transformed to the energy eigenstate basis in order to obtain  $W_{\mathbf{p}\mathbf{p}'}^{\text{eff}}$ , see Eq.(55). The parameter  $r_0$  controls the decay of the scattering potential.  $r_0 = 0$  corresponds to pure *s*-wave scattering, and with  $r_0 p_F \gg 1$  we are in the strong forward scattering limit. For simplicity the strength of the scattering potential and the screening parameter  $r_0$  are here assumed to be independent of  $\omega_s$ . Of course, in order to explain the large magnetoresistance such a dependence has to be taken into account. Suggestions for a microscopic origin of the magnetoresistance have been given, e.g., in Refs. [31–34]. At the end of this section we will also consider the charged impurity scattering, which was discussed in the absence of the spin-orbit coupling, e.g., in [32,33].

Although our main concern here is the anisotropy in the magnetoconductance, it may be useful to begin by

showing the numerical results for the magnetoconductance itself (Fig.8) for the model with a Gaussian scattering probability.

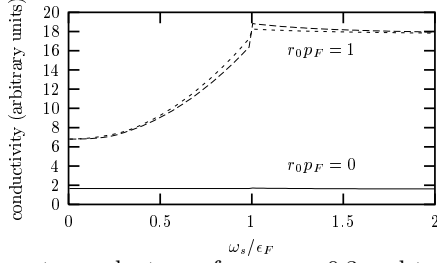


FIG. 8. Magneto-conductance for  $\alpha p_F = 0.3$  and two different screening parameters  $r_0$ . Within the approximations in this section the conductivity is proportional to the inverse of the scattering strength,  $W$ , which we assume here to be independent of the magnetic field. For  $s$ -wave scattering ( $r_0 = 0$ ) the anisotropy of the conductivity is not seen on the scale of the plot. For  $r_0 p_F = 1$  we show the conductivity parallel and perpendicular to the magnetic field.

Given a scattering strength  $W$ , the conductivity increases with the parameter  $r_0$  and with the magnetic field. Both effects are understood easily. The kinematics selects scattering processes with  $q = |\mathbf{p} - \mathbf{p}'| \approx 2p_F$ , whereas the scattering potential of Eq.(73) gives  $q < 1/r_0$ . The condition for effective scattering becomes  $r_0 p_F \ll 1$ . Increasing  $r_0$  weakens the above condition and the conductivity gets enhanced. As a function of the magnetic field the conductivity increases due to a similar reason. The Fermi surface of the lower band grows and the effective condition  $r_0 p_{F,-} \ll 1$  is no longer satisfied.

The numerically determined anisotropy in the magnetoconductance is shown in Fig.9. Since now the conductivity itself is strongly magnetic field dependent we scale  $\Delta\sigma$  with  $\sigma_{xx} + \sigma_{yy}$  instead of  $\sigma_0$ .

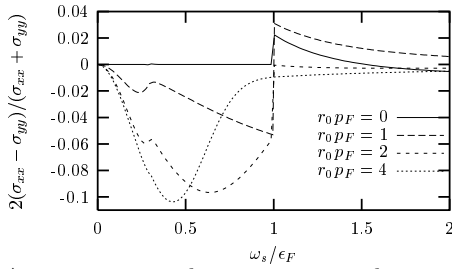


FIG. 9. Anisotropy in the magneto-conductance for  $\alpha p_F = 0.3\epsilon_F$  and varying the screening parameter  $r_0$ . The screening parameters  $r_0 p_F = 1, 2, 4$  correspond to  $\tau_{tr}/\tau \sim 2, 8, 30$  when they are determined for  $\alpha p_F = \omega_s = 0$ .

One observes that the  $p$ -dependent scattering increases the overall size of the anisotropy up to a factor  $\sim 5$  compared to the  $s$ -wave case. The sign of the anisotropy also changes. The peak anisotropy is still at magnetic fields of the order of the Fermi energy, but there is a weak dependence on the scattering potential. The anisotropy as a function of spin-orbit energy is shown in Fig.10. The

overall amplitudes of the various curves are scaled in order to make them more comparable. Also as a function of spin-orbit energy the position of the peak changes only weakly.

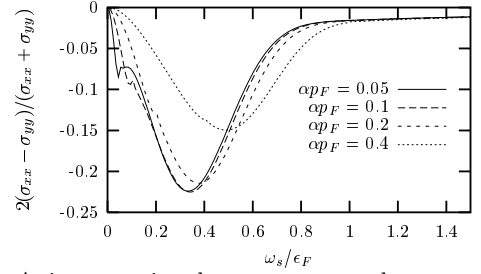


FIG. 10. Anisotropy in the magneto-conductance for strong forward scattering ( $r_0 p_F = 4$ ) for different strengths of spin-orbit scattering. The curves for  $\alpha p_F/\epsilon_F = 0.2, 0.1, 0.05$  are multiplied by 4, 8, 16.

Finally let us consider charged impurity scattering. This type of scattering may explain certain aspects of the magnetoresistance [32]. For a charged impurity situated in the plane the scattering potential is

$$U(q) = 2\pi e^2/[q\epsilon(q)], \quad (74)$$

where  $\epsilon(q)$  is the dielectric function. We approximate it here as

$$\frac{1}{\epsilon(q)} = \frac{1}{1 + (2\pi e^2/q)\chi(q)} \quad (75)$$

where  $\chi(q)$  is the two-dimensional Lindhard function. It has been argued in Ref. [32] that the screening wave number  $q_s = 4\pi e^2 N(\epsilon_F)$  is for low electron density large compared to the Fermi wavelength with the consequence that

$$U(q) \approx \frac{1}{\chi(q)}. \quad (76)$$

The scattering probability is approximated according to  $W(q) \propto |U(q)|^2$ .

In Fig.11 we show the resistivity obtained with  $\alpha p_F = 0.2$  and  $0.4\epsilon_F$ .

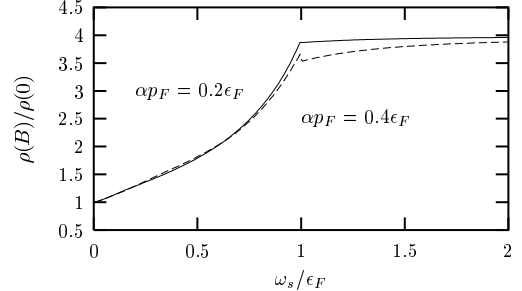


FIG. 11. Resistivity versus in plane magnetic field for charged impurity scattering.

The resistivity increases by a factor of four from the zero field limit to very strong magnetic fields. In the absence of spin-orbit coupling the resistivity saturates when  $\omega_s > \epsilon_F$ , where only one Fermi surface is left [32]. In the presence of spin-orbit coupling there remains a weak increase of the resistivity up to higher magnetic fields, since the depopulation of one band is no more equivalent with the full spin polarization.

The anisotropy in the magnetoresistance for charged impurity scattering is shown in Fig.12.

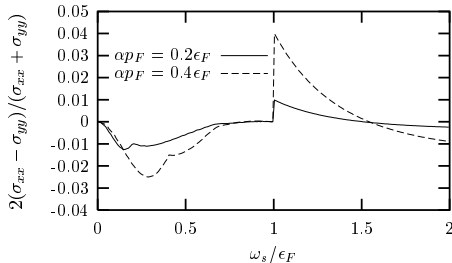


FIG. 12. Anisotropy in the magnetoconductivity versus in plane magnetic field for charged impurity scattering. The strength of the spin-orbit field is  $\alpha p_F = 0.2, 0.4\epsilon_F$ .

Within the approximation adopted the scattering probability depends only weakly on the momentum. Therefore results for the anisotropy are in the intermediate way between the  $s$ -wave and the strong forward scattering limit.

## VI. DISCUSSION

We have calculated the Drude conductivity for a two-dimensional Fermi gas with spin-orbit coupling. In the presence of an in-plane magnetic field the conductivity parallel and perpendicular to the field are different.

Such an anisotropy has recently been observed in Si-MOSFETs [22]. For the range of densities in the experiment  $n_s \approx 0.7 - 1.3 \times 10^{11}/\text{cm}^2$ , the Fermi energy is  $\epsilon_F \sim 5.1 - 9.5\text{K}$ . Taking  $\alpha \approx 6 \times 10^{-6}\text{Kcm}$  which is reported in Ref. [22], the dimensionless spin-orbit parameter is of the order  $\alpha p_F/\epsilon_F \sim 0.3 - 0.7$ . From our theory one expects a relative anisotropy in the magnetoconductance of the order of several percent, in agreement to what is seen experimentally. The maximum anisotropy appears for magnetic fields of the order  $\omega_s \sim \epsilon_F$ , so the peak energy scales with the density, which again agrees with the experiments. We found that the details of the effect depend on the scattering potential. In the case of pure  $s$ -wave scattering the maximum anisotropy appears precisely at the magnetic field, where the upper band depopulates. The conductivity is larger when it is measured parallel to the magnetic field. On the other hand, at higher fields,  $\omega_s > \epsilon_F$ , the conductivity is larger when measured perpendicular to the magnetic field. The sign of the anisotropy at low fields is at odds with the

experiment. Allowing a finite range of the scattering potential, we have shown that the anisotropy sign changes. In particular, in the case of small-angle scattering both the sign and the peak position agree with what is found experimentally. For the case of charged-impurity scattering we found – within the random-phase-approximation – a rather complex pattern of the anisotropy. There are two peaks with opposite sign, one peak near  $\omega_s \sim \alpha p_F$  and the other at  $\omega_s \sim \epsilon_F$ . These results however should be taken with caution when comparing with experiments for the low density electron gas.

Comparison with experiments in heterostructures is even more delicate due the intrinsic crystallographic anisotropies. In both the experiments reported in [25,26] the anisotropy was measured along two crystallographic directions with different mobilities and most likely with different operating scattering mechanisms. At low densities (close and across the MIT) the anisotropy shows  $\Delta\sigma < 0$ , while at high densities there is a change of sign as function of the magnetic field:  $\Delta\sigma < (>)0$  for low (high) fields. In our opinion, while a comparison with the sign of the anisotropy contains the uncertainty related with the knowledge of the scattering mechanism, the fact that the maximum anisotropy at low and moderate fields scales with the density appears as a robust feature in agreement with our theory.

In summary we think that the physics described in this paper may explain the anisotropic magnetoresistance observed in Ref. [22] in Si-MOSFETs, and perhaps that in heterostructures [25,26]. At more general level, our results give a further hint that the Drude-Boltzmann theory is a good starting point for the description of the transport properties of the metallic phase of the 2D electron gas, even near the observed transition to an insulator.

We acknowledge fruitful discussions with C. Castellani and V. Falko. This work was supported by the DFG through SFB 484 and by EU Research Training Network program (Project Nr: RTN1 - 1999-00406).

## APPENDIX A: WARD IDENTITY

In this appendix we derive for the sake of completeness the Ward identities for the system with spin-orbit coupling. The generalized continuity equation is

$$\partial_t \rho(\mathbf{x}, t) + \partial_i \Gamma^i(\mathbf{x}, t) = 0 \quad (\text{A1})$$

where  $i = x, y, z$ . The density and the current operators are

$$\rho(\mathbf{x}, t) = \psi^\dagger_\alpha(\mathbf{x}, t) \psi_\alpha(\mathbf{x}, t), \quad (\text{A2})$$

$$\Gamma^i(\mathbf{x}, t) = \frac{i}{2m} [(\partial_i \psi^\dagger_\alpha(\mathbf{x}, t)) \psi_\alpha(\mathbf{x}, t) - \psi^\dagger_\alpha(\mathbf{x}, t) (\partial_i \psi_\alpha(\mathbf{x}, t))]$$

$$\begin{aligned}
& -\psi_\alpha^\dagger(\mathbf{x}, t)(\partial_i \psi_\alpha(\mathbf{x}, t))] \\
& -\alpha \epsilon_{ijk} n_j \psi_\alpha^\dagger(\mathbf{x}, t) \sigma_{k, \alpha\beta} \psi_\beta(\mathbf{x}, t).
\end{aligned} \tag{A3}$$

Define now the vertex functions

$$\begin{aligned}
\Lambda_{\alpha\beta}^0 &= \langle T_t \rho^i(\mathbf{x}, t) \psi_\alpha(\mathbf{x}', t') \psi_\beta^\dagger(\mathbf{x}'', t'') \rangle \\
\Lambda_{\alpha\beta}^i &= \langle T_t \Gamma^i(\mathbf{x}, t) \psi_\alpha(\mathbf{x}', t') \psi_\beta^\dagger(\mathbf{x}'', t'') \rangle,
\end{aligned} \tag{A4}$$

for which the Ward identities read

$$\begin{aligned}
& \partial_t \Lambda_{\alpha\beta}^0 + \partial_i \Lambda_{\alpha\beta}^i \\
&= \delta(t - t'') \delta(\mathbf{x} - \mathbf{x}'') i G_{\alpha\beta}(\mathbf{x}' t'; \mathbf{x}, t) \\
& - \delta(t - t') \delta(\mathbf{x} - \mathbf{x}') i G_{\alpha\beta}(\mathbf{x} t; \mathbf{x}'' t'').
\end{aligned} \tag{A5}$$

After Fourier transform one gets

$$\omega \Lambda_{\alpha\beta}^0 - q_i \Lambda_{\alpha\beta}^i = G_{\alpha\beta}(p_+, \epsilon_+) - G_{\alpha\beta}(p_-, \epsilon_-). \tag{A6}$$

In the static limit  $\omega = 0$  and letting  $\mathbf{q} \rightarrow 0$  one gets

$$\Lambda_{\alpha\beta}^i = -G_{\alpha\sigma}(p, \epsilon) J_{\sigma\sigma'}^i(p, 0) G_{\sigma'\beta}(p, \epsilon) = -\frac{\partial}{\partial p^i} G_{\alpha\beta}(p, \epsilon). \tag{A7}$$

The above equation is sufficient to see the cancellation of the diamagnetic term in the conductivity, see Eq.(19).

$$\begin{aligned}
& i \sum_{\mathbf{p}} \int_{-\infty}^{\infty} \frac{d\epsilon}{2\pi} \text{Tr} [j^i(p) G(p) J^j(p) G(p)] - \frac{N}{m} \delta_{ij} \\
&= i \sum_{\mathbf{p}} \int_{-\infty}^{\infty} \frac{d\epsilon}{2\pi} \text{Tr} \left[ j^i(p) \frac{\partial}{\partial p^i} G(p) \right] - \frac{N}{m} \delta_{ij} \\
&= -i \sum_{\mathbf{p}} \int_{-\infty}^{\infty} \frac{d\epsilon}{2\pi} \text{Tr} \left[ \frac{\partial}{\partial p^i} j^i(p) G(p) \right] - \frac{N}{m} \delta_{ij} \\
&= -i \frac{1}{m} \delta_{ij} \sum_{\mathbf{p}} \int_{-\infty}^{\infty} \frac{d\epsilon}{2\pi} \text{Tr} [G(p)] - \frac{N}{m} \delta_{ij} = 0
\end{aligned} \tag{A8}$$

In the dynamic limit on the other hand  $q = 0$ ,  $\omega \rightarrow 0$ , Eq.(A6) becomes

$$\omega \Lambda_{\alpha\beta}^0 = G_{\alpha\beta}^R - G_{\alpha\beta}^A, \tag{A9}$$

which can only be solved if the density vertex  $\Lambda^0$  is singular in the zero frequency limit. To see how this translates for the irreducible vertex  $\Gamma$ , write  $\Lambda_{\alpha\beta}^0 = G_{\alpha\sigma} \Gamma_{\sigma\sigma'} G_{\sigma'\beta}$  and perform the  $\mathbf{p}$ -summation on both sides of Eq.(A9). After decomposing in the Pauli matrices components, one gets

$$\omega \left( \begin{pmatrix} \Gamma_0 \\ \Gamma_1 \end{pmatrix} - \begin{pmatrix} \gamma_0 \\ \gamma_1 \end{pmatrix} \right) = i \begin{pmatrix} 1/\tau_0 \\ 1/\tau_1 \end{pmatrix} \tag{A10}$$

where we have used Eqs.(39). From Eq.(A10) one sees that both  $\Gamma_0$  and  $\Gamma_1$  have to be singular in the zero frequency limit.

## APPENDIX B: BOLTZMANN EQUATION

We now briefly demonstrate the equivalence of the approach in section V with the Boltzmann equation. Since we have in mind to solve the Boltzmann equation in the presence of a DC electric field, the distribution function  $g_{\mathbf{p}\alpha}$  is chosen to depend only on the wave vector  $\mathbf{p}$ . The Boltzmann equation including elastic scattering is then written in the form

$$-\mathbf{e} \mathbf{E} \cdot \nabla g_{\mathbf{p}\alpha} = - \sum_{\mathbf{p}'\beta} Q_{\mathbf{p}\alpha, \mathbf{p}'\beta} (g_{\mathbf{p}\alpha} - g_{\mathbf{p}'\beta}). \tag{B1}$$

The Greek indices  $\alpha$  and  $\beta$  label the two spin subbands. The scattering kernel, in the case of elastic scattering, is related to the scattering probability by

$$Q_{\mathbf{p}\alpha, \mathbf{p}'\beta} = 2\pi \delta(E_{\mathbf{p}\alpha} - E_{\mathbf{p}'\beta}) W_{\mathbf{p}\alpha, \mathbf{p}'\beta}^{\text{eff}} \tag{B2}$$

A solution of the linearized Boltzmann equation is looked for in the form

$$g_{\mathbf{p}\alpha} = f(E_{\mathbf{p}\alpha}) + \frac{\partial f}{\partial E} \mathbf{e} \mathbf{E} \cdot \mathbf{u}_{\mathbf{p}\alpha}, \tag{B3}$$

where the vector function  $\mathbf{u}_{\mathbf{p}\alpha}$  obeys the integral equation

$$\mathbf{v}_{\mathbf{p}\alpha} = \sum_{\mathbf{p}'\beta} Q_{\mathbf{p}\alpha, \mathbf{p}'\beta} (\mathbf{u}_{\mathbf{p}\alpha} - \mathbf{u}_{\mathbf{p}'\beta}). \tag{B4}$$

Finally, the electrical current density is given by

$$\mathbf{j} = -e \sum_{\mathbf{p}, \alpha} \mathbf{v}_{\mathbf{p}\alpha} g_{\mathbf{p}\alpha}, \tag{B5}$$

which becomes

$$\mathbf{j} = e^2 \sum_{\mathbf{p}\alpha} \left( -\frac{\partial f}{\partial E} \right) \mathbf{v}_{\mathbf{p}\alpha} (\mathbf{u}_{\mathbf{p}\alpha} \cdot \mathbf{E}). \tag{B6}$$

To make contact with the diagrammatic approach we write

$$\mathbf{u}_{\mathbf{p}\alpha} = \mathbf{J}_{\mathbf{p}\alpha} \tau_{\mathbf{p}\alpha}. \tag{B7}$$

with

$$\tau_{\mathbf{p}\alpha}^{-1} = \sum_{\mathbf{p}'\beta} Q_{\mathbf{p}\alpha, \mathbf{p}'\beta}. \tag{B8}$$

The vector function  $\mathbf{J}_{\mathbf{p}\alpha}$  is the renormalized current vertex, which arises in the diagrammatic approach. This is easily seen in the  $T = 0$  limit, by observing that

$$-\frac{\partial f}{\partial E} \rightarrow \delta(\mu - E_{\mathbf{p}\alpha}) \approx \frac{1}{2\pi} \frac{1}{\tau_{\mathbf{p}\alpha}} G_{\mathbf{p}\alpha}^R G_{\mathbf{p}\alpha}^A. \tag{B9}$$

Upon using  $\mathbf{u}_{\mathbf{p}\alpha} = \mathbf{J}_{\mathbf{p}\alpha} \tau_{\mathbf{p}\alpha}$  and Eq.(B9), the integral equation (B4) becomes

$$\mathbf{J}_{\mathbf{p}\alpha} = \mathbf{v}_{\mathbf{p}\alpha} + \sum_{\mathbf{p}',\beta} W_{\mathbf{p}\alpha,\mathbf{p}'\beta}^{\text{eff}} G_{\mathbf{p}\alpha}^R G_{\mathbf{p}\alpha}^A \mathbf{J}_{\mathbf{p}'\beta} \quad (\text{B10})$$

Hence the linearized Boltzmann equation is equivalent to the approach in section V, where we neglect lifetime broadening.

- 
- [1] S.V. Kravchenko, W.E. Mason, G.E. Bowker, J.E. Furneaux, V.M. Pudalov, and M. D'Iorio, Phys. Rev. B **51**, 7038 (1995).
  - [2] E. Abrahams, S.V. Kravchenko, and M.P. Sarachik, Rev. Mod. Phys. **73**, 251 (2001).
  - [3] B.L. Altshuler, D.L. Maslov, and V.M. Pudalov, cond-mat/0003032.
  - [4] W. Mason, S.V. Kravchenko, G.E. Bowker, and J.E. Furneaux, Phys. Rev. B **52**, 7857 (1995).
  - [5] R. Fletcher, V.M. Pudalov, A.D.B. Radcliffe, and C. Posanzini, cond-mat/0002436.
  - [6] A.M. Finkel'stein, JETP **57**, 97 (1983).
  - [7] C. Castellani, C. Di Castro, P.A. Lee, and M. Ma, Phys. Rev. B **30**, 527 (1984).
  - [8] V. Dobrosavljević, E. Abrahams, E. Miranda, and S. Chakravarty, Phys. Rev. Lett. **79**, 455 (1997).
  - [9] C. Castellani, C. Di Castro, and P.A. Lee, Phys. Rev. B **57**, R9381 (1998).
  - [10] A. Punnoose, A. M. Finkel'stein, cond-mat/0105471.
  - [11] T. Okamoto, K. Hosoya, S. Kawaji, and A. Yagi, Phys. Rev. Lett. **82**, 3875 (1999).
  - [12] S.V. Kravchenko, A.A. Shashkin, D.A. Bloore, and T.M. Klapwijk, Solid State Commun. **116**, 495 (2000) (cond-mat/0007003); A.A. Shashkin, S.V. Kravchenko, V.T. Dolgoplov, and T.M. Klapwijk, cond-mat/0007402.
  - [13] D. Simonian, S.V. Kravchenko, M.P. Sarachik, and V.M. Pudalov Phys. Rev. Lett. **79**, 2304 (1997).
  - [14] V.M. Pudalov, G. Brunthaler, A. Prinz, and G. Bauer JETP Lett. **65**, 932 (1997).
  - [15] S.C. Dultz, and H.W. Jiang, Phys. Rev. Lett. **84**, 4689 (2000) (cond-mat/9909314); S. Ilani, A. Yacoby, D. Mahalu, and H. Shtrikman, cond-mat/9910116.
  - [16] V.M. Pudalov, G. Brunthaler, A. Prinz, and G. Bauer, Phys. Rev. B **60**, R2154, (1999); JETP Lett. **70**, 48 (1999).
  - [17] M. Y. Simmons, A. R. Hamilton, M. Pepper, E. H. Linfield, P. D. Rose, and D. A. Ritchie, Phys. Rev. Lett. **84**, 2489 (2000) .
  - [18] V. Senz, *et al*, Phys. Rev. Lett. **85**, 4357 (2000).
  - [19] B. L. Altshuler, G.W. Martin, D.L. Maslov, V.M. Pudalov, A. Prinz, G. Brunthaler, G. Bauer cond-mat/0008005.
  - [20] V.M. Pudalov, JETP Lett. **66**, 175 (1997).
  - [21] Guang-Hong Chen, M.E. Raikh, and Yong-Shi Wu, Phys. Rev. B **61**, R10539 (2000).
  - [22] V.M. Pudalov, G. Brunthaler, A. Prinz, and G. Bauer, cond-mat/0004206.
  - [23] R. Raimondi, M. Leadbeater, P. Schwab, E. Caroti, and C.Castellani, cond-mat/0101473.
  - [24] V.S. Khrapai, E.V. Deviatov, A.A. Shashkin, and V.T. Dolgoplov, cond-mat/0005377.
  - [25] S.J. Papadakis, E.P. De Portere, M. Shayegan, and R. Winkler, Phys. Rev. Lett. **84**, 5592 (2000).
  - [26] H. Noh, J. Yoon, D.C. Tsui, and M. Shayegan, cond-mat/0104240.
  - [27] Y.A. Bychkov and E. I. Rashba, JETP Lett. **39**, 78 (1984).
  - [28] R. Winkler, Phys. Rev. B **62**, 4245 (2000).
  - [29] A.A. Abrikosov, L.P. Gorkov, and I.E. Dzyaloshinski "Methods of Quantum Field Theory in Statistical Physics" Dover Publications, New York (1963).
  - [30] R.N. Bhatt, P. Wölfle, and T.V. Ramakrishnan, Phys. Rev. B **32**, 569 (1985).
  - [31] S. Das Sarma and E.H. Hwang, Phys. Rev. Lett. **84**, 5596 (2000).
  - [32] V.T. Dolgoplov and A. Gold, JETP Lett. **71**, 27 (2000).
  - [33] A. Gold, JETP Lett. **72**, 274 (2000).
  - [34] I.F. Herbut, Phys. Rev. B **63**, 113102 (2001).